Impact of conventional and modified ring spun yarn structures on the generation and release of fragmented fibres (microfibres) during abrasive wear and laundering

Impact of conventional and modified ring spun yarn structures on the generation and release of fragmented fibres (microfibres) during abrasive wear and laundering

Abdul Jabbar [a, b], Alma V. Palacios-Marín[a], Ali Ghanbarzadeh[c], Dongmin Yang[d], *Muhammad Tausif* [a, *]

[a] School of Design, University of Leeds, Leeds, LS2 9JT, United Kingdom.

[b] Department of Textile Engineering, National Textile University, Faisalabad-37610, Pakistan

[c] School of Mechanical Engineering, University of Leeds, Leeds, LS2 9JT, United Kingdom.

[d] School of Engineering, University of Edinburgh, Edinburgh, EH9 3FB, United Kingdom.

* Corresponding author

Dr Muhammad Tausif, School of Design, University of Leeds, Leeds, LS2 9JT, UK.

Phone: +44(0)113 343 3799, Email: m.tausif@leeds.ac.uk

Abstract

The abrasive wear of textiles during ordinary use and laundering results in fibre damage which leads to the generation and release of fragmented fibres (FF). Ring spun yarn has a dominant share of about 70% of global spun yarn production. The effect of conventional and modified ring yarn structures (Compact, SIRO and SIRO-compact) on FF release from cotton textiles during repeated abrasion and laundering was studied. All prepared cotton yarns and textiles are industrially and commercially relevant. The FF formed during each abrasion and washing cycle were collected from textiles and quantified. The yarn tensile properties and

fabric frictional characteristics were employed to explain the release of FF. For the first time, the morphology of collected fragmented fibre ends was associated with the fibre damage nature (granulated and fibrillated) induced by different types of stresses and experimental exposure conditions. The results demonstrated that modified ring yarn structures had released significantly less FF mass as compared to conventional ring yarn structures. The tensile strength was decreased, and breaking elongation increased after repeated abrasion and washing. The fabric surface properties were also affected by abrasion and laundering. The yarn structure choices impact the amount of released fragmented fibres, which are dispersed into the environment as a pollutant or a carrier of pollutants with potential hazards to the health of the environment and living organisms.

Keywords: Fragmented fibres; microfibres; microplastics; modified ring yarns; Martindale abrasion; fibre damage

1 Introduction

The release of fragmented fibres (FF), from both natural (1, 2) and manufactured (3-6) textiles, is an established source of anthropogenic pollution in the aquatic and terrestrial environment. A fibre fragment is a short textile fibre (typically < 5.0 mm long) (7) broken or separated away from a textile construction. The term ‘microfibre’ has also been commonly used to describe fibrous and/or microplastic pollution from textiles. Textiles are known to shed FF during production (8), everyday use (9), laundering (9-16) and drying (17-19), but also continue to release FF after disposal (20). In 2018, global fibre production reached 111 million tons (21) and is expected to grow at the rate of 3.7% per annum reaching 130 million tons by 2025 (22). Among textile fibres, polyester and cotton are the dominant fibres used in the global production of textiles, with an approximate share of 54.5% and 24.3% in global fibre production, respectively (21). Polyester is a synthetic polymer fibre, whereas cotton is a natural cellulosic fibre. The rising clothing demand due to the increasing world population

and fast fashion trends are the main reasons responsible for the increase in global fibre production and textiles consumption (23), which ultimately leads to an rise in anthropogenic pollution.

Several studies have reported polyester textiles as a dominant source of anthropogenic pollution (10, 13, 24-27). However, the presence of both natural and synthetic fibres in the environment has been reported. Despite some studies have shown cotton fibres biodegradable in fresh water and marine environment (28, 29) there are still some concerns in published literature about the fate and role of natural fibres in the aquatic environment (3, 30, 31). For example, the presence of colorants and other chemical additives in cotton textiles modifies the chemical nature of natural cellulose, which may complicate the biodegradation process and aquatic toxicity of these microfibres in the marine environment (32). A recent study discloses that cotton fabrics dyed with reactive dye or treated with water repellent finish are less biodegradable in seawater than untreated cotton specimens (33). Athey *et al*. (1) identified the presence of modified cellulose microfibres, originating from indigo dyed cotton denim jeans, in aquatic environments serving as a tangible and potent indicator of anthropogenic pollution.

Staple spun yarns account for some 45% of global yarn production (34) with cotton being a leading fibre consumed in the spun yarn industry (35). Ring spinning is the dominant technology (despite being nearly 200 years old) in the spun yarn industry with a share of about 70% of global spun yarn production technologies (36) due to better suitability of the ring-spun yarn structure and properties to a wide range of textile applications (37). Since the invention of ring spinning, it has gone through many developments to increase the productivity of conventional systems and improve the quality of ring spun yarn. Among different advancements, modified ring spinning systems (especially Compact, SIRO and SIRO-compact) have brought substantial modifications to the conventional ring spinning

process with the aim of changing the structural arrangement of fibres in the yarn (38). The better structural integrity of fibres in the yarn may result in improved fibre cohesion within the yarn structure, which may contribute to less fabric wear during ordinary everyday use and laundering, and hence less release of FF during the whole service life of textiles. The schematic representation of differences in yarn formation principle of mentioned ring spun yarns are shown in Figure 1. Briefly, the conventional and modified ring spinning systems have the main difference in the geometry of the yarn formation zone i.e., the spinning triangle, which results in the different structural arrangement of fibres in the yarn. The conventional ring spinning has a normal spinning triangle whose width depends on the width of the drafted fibre strand and spinning tension during yarn formation. In compact spinning, the width of the spinning triangle is significantly reduced due to condensing of fibre strands before yarn formation. In SIRO-spinning, the main spinning triangle is divided into two primaries and one final spinning triangle by feeding two rovings in parallel at a predetermined spacing through the drafting unit. In SIRO-compact spinning, both the compact and SIRO spinning principles are combined.

Textiles wear out and release FF mainly due to abrasive wear and breakage of textile fibres during manufacturing, use and laundering (32). In textiles, the wear of fibres, yarns, and fabrics is caused by a rubbing action which involves relative motion between two fabric surfaces or a fabric surface and another material (39). There are different parameters which influence the generation and release of FF from textiles, including physicochemical properties of textile fibres and their morphology, yarn type and structure, fabric type and geometry, and textile processing history (32). De Falco *et al*. (9) disclosed the lowest release of FF from textiles with a very compact woven structure and highly twisted yarns made of continuous filaments compared to that of an open structure. Balasaraswathi *et al*. (40) studied the effect of knitted fabric structure and fabric mass areal density on FF shedding from 100%

polyester textiles. It was reported that interlock knitted structures shed more FF during laundry compared to 1×1 rib and single jersey structures. Furthermore, fabric structural parameters such as higher stitch density, higher tightness factor, lower loop length, and less fabric mass areal density resulted in reduced FF shedding. A recent study elucidated the impact of key yarn structures and material composition on the number of released FF and the fibre length distribution profile (41). Similarly, another study reported the influence of fabric geometrical parameters on FF release (42).

In a correlation study to compare the actual fabric wear with laboratory abrasion and laundering, the laboratory abrasion followed by laundering reproduced very similar results to actual wear of fabric during ordinary use compared to laboratory abrasion or laundering alone (43). Therefore, the objective of the present study is to understand the influence of ring spinning variants (Conventional, Compact, SIRO and SIRO-compact) on the release of FF from textile fabrics by simulating fabric wear during ordinary use with laboratory abrasion followed by laundering processes. For the first time, released FF fibre ends morphology was studied and associated with the number of exposure cycles. The outcome of this study will not only help to give an insight into the effect of the structural arrangement of fibres in the yarn on the release of FF from textiles, but also provide insights on yarn structural choices to mitigate the generation of FF released during wearing and laundering. This can help to at-source decrease the release of FF in both dry and wet environments, compared to the end-of-pipe approaches to capture the released FF, which are mainly designed for released FF during laundering.

2 Materials and methods

2.1 Yarn and fabric preparation

Four types of carded ring spun yarns including Conventional, Compact, SIRO and SIRO compact, were produced using PIMA cotton as listed in Table 1. The raw cotton fibres were processed through a blow room line (Toyoda-Ohara-Hergeth), carding machine (Howa CM80), breaker drawing frame (Toyoda DYH 500C), finisher drawing frame (RSB D40), roving frame (Toyota FL-16), ring frame (Toyota RY-5 for normal and SIRO yarns and Rieter K-44 for compact and SIRO compact yarns) to produce carded ring spun yarns of linear density 14.76 Tex (40.0 Ne) having a nominal twist level of 10.71 turns.cm^{-1} (27.20 turns.inch^{-1}) in all samples. The properties of produced yarns are given in Table 2. The yarns were converted into a plain-woven fabric with thread densities of 35.43 threads cm^{-1} (90 threads inch^{-1}) in warp direction and 29.92 threads.cm^{-1} (76 threads inch^{-1}) in weft direction on a sample rapier-weaving loom by CCI Tech Incorporated Taiwan. The warp yarns were treated (sized) with polyvinyl alcohol (PVA) solution before weaving to reduce thread breakages during the weaving process. The fabric samples were named Conventional, Compact, SIRO and SIRO-compact based on the yarn.

2.2 Fabric pre-treatment and dyeing

The fabric samples were washed with 1.0 g.l^{-1} Invadine® PBN at 80 °C for 45 min maintaining a liquor ratio of 10:1 and scoured and bleached in a single step using 1.5% w/w NaOH and 5.0% v/w H_2O_2 at 80 °C for 90 min with a liquor ratio of 5:1 followed by rinsing, neutralisation and drying at room temperature for 24 h. To identify any cross-contamination, the bleached fabrics were dyed into four different colours by exhaust method using Remazol Red 3B for Conventional fabric, Remazol Golden Yellow RGB for Compact, Remazol Brilliant Blue BB for SIRO and Remazol Black B for SIRO-compact fabrics. The dyeing process was carried out at 1% owf of each dye in 80 g.l^{-1} NaCl and 20 g.l^{-1} Na_2CO_3 at 60 °C

with a liquor ratio of 20:1 according to dyeing procedure presented in Figure 2. The fabrics were washed with 0.5 $g.l^{-1}$ Invadine® PBN at 100 °C for 30 min and then rinsed thoroughly with tap water, neutralised, and dried again at room temperature.

2.3 Sample preparation for Martindale abrasion

The study aimed to simulate the fabric wear during ordinary use by employing multiple cycles of rubbing and subsequent laundering to understand the influence of four different ring-spun yarn structures on the release of FF from textiles. The fabric-to-fabric rubbing was carried out on a Martindale abrasion tester (James Heal 5-station Martindale abrasion tester, model 1305). The fabric samples were cut into square sizes of 6.5×6.5 cm^2 (Specimen) and 16×16 cm^2 (Abradant) from the same fabric sample. Using Coats Astra (Tkt 120, 13ANT) 27 Tex 100% staple spun polyester thread of light green colour, the samples were overlocked, folded 0.5 cm from each side, and sewn using the same thread. The overlocking/sewing thread colour was intentionally different from colours of the textile samples to differentiate any release of FF from the sewing thread (41). The final sizes of Specimen and Abradant were 5.5×5.5 cm^2 and 15×15 cm^2. Textile manufacturing processes involve fibre-fibre, fibre-metal, and fibre-water interactions, which are known to cause fibre damage, leading to a higher amount of FF generation in the first cycle (41). Hence, all samples were subjected to a prewashing step, without using any steel balls, to collect FF associated with textile manufacturing and to remove any contaminants, excess dye, dust and dirt particles. The prewashing was carried out at 40 °C for 45 min at 40 rpm in a standardised laboratory laundry equipment (GyroWash, James Heal) using 100 and 250 ml of distilled water for Specimen and Abradant, respectively. The steel canisters were thoroughly washed with distilled water before washing operation. A 2.7% omf of AATCC high-efficiency standard reference liquid detergent without optical brightener was added in distilled water for

prewashing of samples. After prewashing, the samples were rinsed with distilled water thoroughly and dried in an oven at 50 °C overnight.

2.4 Martindale abrasion and collection of FF

As per ISO-12974:2, a preliminary abrasion test was conducted, and the abrasion resistance was found to be 3500-4000 rubs for the fabrics under study. Since the current study is aimed to simulate the actual fabric wear during ordinary use a repeated laboratory abrasion followed by laundering cycles was employed to understand the influence of selected ring yarn structures on the release of FF from textiles. The Specimen was abraded to 500 rubs against the Abradant by applying 12kPa pressure. The abrasion experiment was stopped after 500 rubs, and both Specimen and Abradant were separately subjected to washing. This abrasion & laundering cycle was repeated six times, and FF were collected during each cycle separately from the Specimen and the Abradant. ISO-12974:2 standard was modified as per (27) to avoid cross-contamination of the collected FF and the modified experimental setup is shown in Figure 3. As a substitute to underlay polyurethane foam and woven felt, rubber sheets of 1.0 mm thickness were used. Furthermore, the same test textile as the Specimen was replaced with a standard abradant (woven wool fabric) to simulate the same fabric-on-fabric abrasion. It has been recognised in (27) that mounting a cylinder on each abrasion station does not allow the escape of FF generated during abrasion experiment, so an acrylic Perspex cylinder, having height 50 mm, inner diameter 140 mm and thickness 5 mm, was mounted around each of the test stations to collect generated FF and to avoid cross contamination between samples during abrasion test.

After each cycle (abrasion & laundering), the apparatus parts (Perspex ring, rubber underlay and metallic sample holders) exposed to Specimen and Abradant were rinsed three times using distilled water separately, and the effluent was recovered for subsequent filtration. The FF were collected from textile samples (Specimen and Abradant) separaely by employing the

same laundering procedure outlined in section 2.3. Post laundering, the effluent was collected in a beaker. A pair of tweezers was used to remove excess water from the textile samples, and the detergent foam was removed by rinsing the specimen in distilled water. The open mesh, beakers, and tweezers were rinsed three times. All recovered effluent from apparatus parts, laundering, and rinsing the textile samples was then collected in one beaker for subsequent filtration. The laundered samples were left to dry in a fan oven for a minimum of 4 hours at 50 °C and then conditioned again for the next abrasion & laundering cycle. The beaker and glass funnel were also rinsed three times, and all the collected effluent was filtered using a binder-free glass fibre filter of 1.6 µm mean pore size and 47 mm diameter (Merck Millipore Ltd. Ireland). The filters were weighed before filtration using a precision balance (Mettler Toledo AE160, resolution of 0.00001 grams). After filtration, the filters were placed in a fan oven overnight at 50 °C, conditioned for 4 hours and re-weighed to determine the increase in filter mass, which corresponds to the amount of released FF from textile samples. The order of experiments was randomised to minimise the chances of systematic error. During the experiments, protective nitrile gloves and a white laboratory coat were worn to minimise any cross-contamination. The experimental order was randomised to minimise the chances of systematic error.

2.5 Testing and characterisation

The yarns were carefully taken out from the warp direction of the Abradant fabric before the start and after the 6^{th} cycle to quantify any change in the tensile properties of yarns during repeated abrasion & laundering. Following, twenty yarn specimens from each fabric sample were tested on a universal testing machine at 100 mm gauge length and with 5kN load cell (Titan, James Heal). The surface roughness and coefficient of friction of Abradant in warp direction (n =4), before the start and after the 6^{th} cycle, were measured using the Kawabata KES-FB4 surface tester to record any changes in surface properties during repeated abrasion

& laundering. The fibre ends of FF collected on glass filters after 1st and 6th abrasion & laundering cycles for Conventional and SIRO-compact fabric samples were analysed using scanning electron microscope (Jeol JSM-6610, Japan) to characterise the types of fibre damage during abrasion and washing. Three filters from each sample were randomly selected and analysed to get 3 to 4 images of damaged fibre ends from each filter to get a total of 10 SEM images. The filters were sputter-coated with a 60μm gold layer by using a sputter coater (Q150RS by Quorum Technologies). Tukey's comparison method, using one-way analysis of variance (ANOVA), was employed to compare the statistical significance of the release of FF mass from the four different fabrics during repeated abrasion & laundering cycles. Student's t-test was used to determine the statistical significance of the results of yarn tensile properties and Kawabata surface properties before start and after 6th abrasion & laundering cycles.

3 Results and discussion

3.1 The release of FF mass during repeated abrasion and laundering

The mass of FF collected from abraded Specimens and Abradants after each of the six abrasion & laundering cycles for each fabric sample is plotted in Figure 4. It is evident that Specimen of Conventional sample releases a higher amount of FF compared to the rest of the samples. This is supported by statistical analysis (Table 3) which shows a significant difference in collected FF mass from Conventional Specimen compared to the remaining three structures for up to the 5th cycle. The fibres undergo fibre-to-fibre and fibre-to-metal friction during textile manufacturing leading to fibre fatigue or fracture (44). The higher release of FF during the first cycle can be associated with the accumulated effect of abrasion and fibre damage during textile manufacturing. For Specimen (Figure 4), this release of FF mass decreases gradually up to the 3rd cycle, and generally there is a steady state behaviour in the subsequent cycles for each textile sample.

For Abradant fabric (Figure 4), generally, there is a consistent release of FF mass in all cycles. This is evident by statistical analysis (Table 3), which shows a significant difference in collected FF mass by Conventional Abradant compared to the remaining three structures only during the first cycle. The Specimens release a higher amount of FF as compared to Abradants for all textile samples after each abrasion & laundering cycle, as shown in Figure 4. During Martindale abrasion process, the exposed area of Specimen is continuously rubbed against the Abradant, so the fibres in the exposed area of Specimen are under continuous tensile and/or shear stresses, leading to more fibre damage and generation of FF irrespective of the type of fibre and yarn/fabric structure. Whereas the fibres in the exposed area of Abradant are intermittently rubbed due to the Lissajous pattern of rubbing (as recommended in standard ISO-12974:2) during Martindale abrasion and hence less fibre damage and generation of FF.

The results demonstrate that textiles produced from Conventional yarn shed more FF compared to textiles produced from Compact, SIRO and SIRO-compact yarns. The yarn structure (i.e., geometrical arrangement and binding of fibres in the yarn) may likely to be an important characteristic, among other factors, affecting the generation and release of FF from textiles. The yarn structure largely depends on fibre migration, and the geometrical arrangement of fibres in staple spun yarns (45). Fibre migration, which is described as the relative movement of a fibre with respect to its neighbouring fibres during yarn formation and its ultimate position in the yarn body (46), affects the compactness (packing fraction) and binding of fibres in the yarn. In the current study, all textile samples were made from ring spun yarns which were produced by conventional and modified ring spinning systems. The modified ring spinning systems, including Compact, SIRO, and SIRO-compact, alter the flow behaviour of fibres in the yarn formation zone and/or the geometry of the spinning triangle at the exit of drafting system which lead to a decisive impact on yarn structure and properties

including higher fibre migration (47), compactness, tenacity and less hairiness (48) as compared to conventional ring spinning. The higher fibre migration and compactness would lead to an increase in inter-fibre friction and cohesive forces holding the fibres together in the yarn. Therefore, the deformation developed in fibres due to induced mechanical stresses during downstream textile production processes and abrasive wear may dissipate largely to neighbouring fibres in the yarn body resulting in comparatively less damage, removal or displacement of fibres and ultimately less generation of FF.

3.2 Tensile properties of yarns

The results of tensile strength and breaking extension of yarns, removed from warp direction of the Abradant samples, before start and after the 6^{th} cycle, are plotted in Figure 5a and 5b, respectively. The tensile strength of yarns decreased while the breaking extension increased for all samples. However, the differences were only significant for Conventional and Compact yarn (Table 4). SIRO and SIRO-compact yarn structures offer higher fibre migration and entanglement of fibres during yarn formation. For example, Soltani *et al*. (47) observed that SIRO spun yarns demonstrate higher migration parameters as compared to compact and conventional ring spun yarns at similar twist levels. The higher fibre migration leads to a coherent self-interlocking yarn structure in which the fibre movement or slippage is restricted (49). Hence, improved yarn structure coupled with significantly less generation of FF during abrasion (Figure 4) may contribute to better retention of tensile strength after repeated abrasion & laundering. The increase in breaking extension is statistically significant for all samples (Table 4). There might be a release of residual stresses among fibres in yarn upon successive abrasion & laundering causing the yarn structure to relax and extend more before breaking. Furthermore. during tensile loading, the applied load is distributed among the fibres in yarn. The yarns in fabric may become weaker during repeated abrasion & laundering, possibly due to fibre fatigue and fibre damage. Subject to repeated abrasion &

laundering, the yarn microstructure is likely to be affected, leading to a change in inter-fibre cohesion and inter-fibre friction. The change in microstructure compounded with fibre damage may lead to the decrease in strength of yarns and an increase in extension at break.

3.3 Evaluation of Surface Friction Coefficient and Roughness

The measured values of KES coefficient of friction (MIU) and surface roughness (SMD) in the warp direction of the Abradant samples before start and after the 6th cycle, are shown in Figure 6a and 6b, respectively. The frictional coefficient is increased for all textile samples, and the increase is statistically significant as shown by the statistical significance values in Table 4. The coefficient of friction is a function of a number of parameters such as material properties, normal force, contact geometries and environmental factors (50). Since the normal force is constant during the abrasion experiment; therefore, the increase in the coefficient of friction after the 6th cycle may be explained by the increase in the surface area in contact. At zero cycles, the contact area between the Specimen and Abradant is assumed to be small. But after repeated abrasion and laundering, FF generated due to frictional wear are extracted and the contact area is supposed to be increased which may be attributed to the increase in the coefficient of friction of textile samples (Figure 6a).

The surface roughness depicts a decrease for Conventional sample but increase for Compact, SIRO and SIRO-compact samples as shown in Figure 6b. Nevertheless, all changes in surface roughness are statistically insignificant (Table 4). Furthermore, the average coefficient of variation of roughness was high, with values of 13.03 % and 10.66 % for zero cycle and after 6th cycle, respectively. This suggests that the Conventional sample is the roughest at zero cycle possibly due to poor fibre alignment, higher yarn hairiness and a higher percentage of folded and entangled fibres in the yarn body (49). In comparison, Compact, SIRO, and SIRO-compact yarns have better fibre orientation and binding of fibres in the yarn body and low hairiness as compared to the normal sample, which can be associated with a low surface

roughness of corresponding textile samples at zero cycle. During frictional wear dominated by an adhesion mechanism, the decrease in surface roughness will result in increased frictional force in contact (51). The continuous higher release of FF from the Conventional sample may be associated to a decrease in amplitude of variation in the surface, resulting in a decrease in surface roughness after 6th cycle. The surface appearance of the Conventional sample after 6th cycle is visible in Figure 7a, which shows noticeable surface abrasion with fibre fuzziness. However, more coherent modified ring yarn structures, with relatively less release of FF than Conventional sample, may offer a more resistance to decrease in amplitude of variation in the fabric surface. For Compact, SIRO and SIRO-compact samples, the presence of some pilling, as witnessed by Figure 7b, c & d respectively, may also be reasoned for the increased amplitude of variation in surface, causing an increase in surface roughness.

3.4 SEM for morphological analysis of fragmented fibre ends

The morphology of fibre ends can be associated to the nature of fibre damage induced by different types of stresses and exposure conditions (52). Hence, the microscopic examination of damaged fibre ends in FF mass was carried out to understand the nature of the failure mechanism of fibres in reference to different yarn structures. SEM examination of collected FF (over glass fibre filter) of Conventional and SIRO-compact Abradant samples after 1st and 6th cycles of abrasion & laundering was performed and presented in Figures 8 and 9, respectively. Ten fibre ends were randomly imaged from the surface of each glass filter of Conventional and SIRO-compact samples. The granulated/transverse damage with a short length of independent fibrils separation (Figures 8a-1, 8b-1, 9a-1, and 9b-1), and fibrillated damage/longitudinal splits (Figure 8a-2, 8b-2, 9a-2 and 9b-2) were found to be the main types of fibre damage. The previous studies suggest that FF/microfibres may already be contained in textiles which could be originated during textile production processes (10, 53). These FF are found to be present in various textile products before the start of their use phase. The

transverse damage ends of FF prominent after the 1st cycle, as shown in Figures 8a-1and 9a-1, may suggest the history of mechanical stresses and high energy cuts induced during textile production processes which are likely to be released from textiles due to their mobilisation from textile structure during the first abrasion & laundering cycle. This may further suggest that the majority of the transverse damaged FF are less likely to be formed during the abrasion process but are only released from the yarn (textile) structure during the 1st exposure cycle (27). Despite the prewashing of textile samples was done in the present study to remove already existing FF in textile structures, but no further steps were undertaken to ensure the removal of textile production associated with FF before starting abrasion & laundering cycles. Therefore, further understanding of the prewashing (such as additional pre-washing steps) is necessary to ensure that all pre-existing FF have been removed. This, aided with the study of the nature of fibre damage by microscopic examination of damaged fibre ends, would help to differentiate between the FF originated by manufacturing or by the exposure cycles..

The magnitude of frictional force between the Specimen and Abradant during the abrasion experiment may be an additional possible influencing factor affecting the type of fibre damage. The Kawabata surface evaluation of Abradant, as shown in Figure 6, highlights that the coefficient of friction is less at initial cycles for all samples, which increases after 6th cycle. This indicates that the frictional wear of textiles samples is dominated by adhesion (51, 54). At the start of abrasion and laundering experiments, contact may occur at the tips of asperities due to surface roughness, and the applied load may be distributed in a small real contact area which may be responsible for rupturing the fibres due to a greater deformation by the development of tensile and shear stresses leading to a transverse damage during abrasion. However, in the remit of this study, it was not possible to differentiate between transversely damaged FF from abrasion process and textile manufacturing.

The abrasion process leads to fibre fatigue, rupture and fibrillation which may result to induce fibrillated damage after the 1st cycle (Figures 8a-2, 9a-2). A relatively strong adhesion between two fabric surfaces, likely due to an increase in the contact area after successive abrasion & laundering, may result in shear failure of fibres under repeated flexing and rotational fatigue, leading to the more yielding and plastic deformation, which may be responsible for interfibrillar slippage and noticeable fibrillated fibre damage (55) with more scattering and progressive cracking paths generally observed after the 6th cycle (Figure 8b-2, 9b-2). Moreover, repeated deflection of surface fibres under the influence of periodic mechanical stresses during rubbing cycles may add to strong fibrillation after repeated abrasion & laundering with rupture of fibres into fine fibrils as shown in Figures 8b-2 and 9b-2. The fibres at or near the fabric surface bear highest stresses, and repeated and periodic rubbing deform surface fibres leading them to fibrillate and ultimately rupture. The fibrils under stress are much finer and therefore less resilient in response to mechanical stresses compared to the non-fibrillated fibres, leading to fibrillated failure of the fibres (56). Apparently, the difference in yarn structure was not found to prominently influence the nature of fibre damage.

4 Conclusions

The conventional and modified (compact, SIRO and SIRO-compact) ring spun yarns were employed to produce dyed woven textiles, which were subjected to simulated repeated laboratory abrasion and laundering to identify the impact of yarn structure on the release of fragmented fibre mass. All other manufacturing parameters were kept constant for direct comparison. It was found that textiles with modified ring yarn structures released significantly less quantity of FF as compared to textile with conventional ring yarn. The tensile strength of yarns (removed from test textiles) was decreased, and breaking elongation increased after repeated abrasion & laundering. However, t-test revealed an insignificant decrease in tensile

strength of SIRO and SIRO-compact yarns, which may be due to more coherent self-interlocking structure of these yarns. The coefficient of friction was increased for all textile samples after repeated abrasion & laundering; however, surface roughness disclosed a decrease for Conventional sample and an increase for Compact, SIRO and SIRO-compact samples after repeated abrasion & laundering. The SEM of damaged fibre ends identified the granulated/ transverse and fibrillated damages as the main types of fibre damages. The transverse damage was evident after 1st abrasion & laundering cycle and fibrillated damage was prominent after 6th cycle. The yarn structure was not apparent to influence the type of fibre damage. This study reveals that the yarn structure choices impact the amount of released fragmented fibres, which in turn, are dispersed into the environment as a pollutant with potential hazard to the health of the environment and living organisms.

5 Acknowledgement

This work was financially supported by the Engineering and Physical Sciences Research Council (EPSRC) of UK under the grant reference number EP/T024542/1 and EP/T02464X/1.

References

1. Athey SN, Adams JK, Erdle LM, Jantunen LM, Helm PA, Finkelstein SA, et al. The widespread environmental footprint of indigo denim microfibers from blue jeans. *Environ Sci Techn Lett* 2020; 7(11): 840-7.
2. Zambrano MC, Pawlak JJ, Daystar J, Ankeny M, Venditti RA. Impact of dyes and finishes on the microfibers released on the laundering of cotton knitted fabrics. *Environ Poll* 2021; 272: 115998.
3. Mishra S, charan Rath C, Das AP. Marine microfiber pollution: a review on present status and future challenges. *Marin Poll Bullet* 2019; 140: 188-97.
4. Henry B, Laitala K, Klepp IG. Microfibres from apparel and home textiles: prospects for including microplastics in environmental sustainability assessment. *Sci Tot Environ* 2019; 652: 483-94.

5. Acharya S, Rumi SS, Hu Y, Abidi N. Microfibers from synthetic textiles as a major source of microplastics in the environment: A review. *Text Res J* 2021; 91: 2136–56.
6. Belzagui F, Crespi M, Álvarez A, Gutiérrez-Bouzán C, Vilaseca M. Microplastics' emissions: Microfibers' detachment from textile garments. *Environ Poll* 2019; 248: 1028-35.
7. Alma V Palacios-Marín, Tausif M. Fragmented Fibre (Including Microplastic) Pollution from Textiles. *Text Prog* 2022; DOI:10.1080/00405167.2022.2066913.
8. Chan CKM, Park C, Chan KM, Mak DCW, Fang JKH, Mitrano DM. Microplastic fibre releases from industrial wastewater effluent: a textile wet-processing mill in China. *Environ Chem* 2021; 18: 93-100.
9. De Falco F, Cocca M, Avella M, Thompson RC. Microfiber release to water, via laundering, and to air, via everyday use: a comparison between polyester clothing with differing textile parameters. *Environ Sci Techn* 2020; 54(6): 3288-96.
10. Cai Y, Mitrano DM, Heuberger M, Hufenus R, Nowack B. The origin of microplastic fiber in polyester textiles: The textile production process matters. *J Clean Prod* 2020; 267: 121970.
11. Cesa FS, Turra A, Checon HH, Leonardi B, Baruque-Ramos J. Laundering and textile parameters influence fibers release in household washings. *Environ Poll* 2020; 257: 113553.
12. De Falco F, Di Pace E, Cocca M, Avella M. The contribution of washing processes of synthetic clothes to microplastic pollution. *Sci Rep* 2019; 9(1): 1-11.
13. Cai Y, Yang T, Mitrano DM, Heuberger M, Hufenus R, Nowack B. Systematic study of microplastic fiber release from 12 different polyester textiles during washing. *Environ Sci Techn* 2020; 54(8): 4847-55.
14. Sillanpää M, Sainio P. Release of polyester and cotton fibers from textiles in machine washings. *Environ Sci Poll Res* 2017; 24(23): 19313-21.
15. Özkan İ, Gündoğdu S. Investigation on the microfiber release under controlled washings from the knitted fabrics produced by recycled and virgin polyester yarns. *J Text Inst* 2021; 112(2): 264-72.
16. Yang L, Qiao F, Lei K, Li H, Kang Y, Cui S, et al. Microfiber release from different fabrics during washing. *Environ Poll* 2019; 249: 136-43.
17. Kapp KJ, Miller RZ. Electric clothes dryers: An underestimated source of microfiber pollution. *Plos One* 2020; 15(10): e0239165.
18. O'Brien S, Okoffo ED, O'Brien JW, Ribeiro F, Wang X, Wright SL, et al. Airborne emissions of microplastic fibres from domestic laundry dryers. *Sci Tot Environ* 2020; 747: 141175.

19. Kärkkäinen N, Sillanpää M. Quantification of different microplastic fibres discharged from textiles in machine wash and tumble drying. *Environ Sci Poll Res* 2021; 28(13) :16253-63.
20. Sun J, Zhu Z-R, Li W-H, Yan X, Wang L-K, Zhang L, et al. Revisiting Microplastics in Landfill Leachate: Unnoticed Tiny Microplastics and Their Fate in Treatment Works. *Water Res* 2021; 190: 116784.
21. Zhang Y-Q, Lykaki M, Alrajoula MT, Markiewicz M, Kraas C, Kolbe S, et al. Microplastics from textile origin–emission and reduction measures. *Green Chem* 2021; 23: 5247-71.
22. Dahlbo H, Aalto K, Eskelinen H, Salmenperä H. Increasing textile circulation—consequences and requirements. *Sustain Prod Consum* 2017; 9: 44-57.
23. Koszewska M. Circular economy—Challenges for the textile and clothing industry. *Aut Res J* 2018; 18(4): 337-47.
24. Browne MA, Crump P, Niven SJ, Teuten E, Tonkin A, Galloway T, et al. Accumulation of microplastic on shorelines woldwide: sources and sinks. *Environ Sci Techn* 2011; 45(21): 9175-79.
25. Hernandez E, Nowack B, Mitrano DM. Polyester textiles as a source of microplastics from households: a mechanistic study to understand microfiber release during washing. *Environ Sci Techn* 2017; 51(12): 7036-46.
26. Dalla Fontana G, Mossotti R, Montarsolo A. Assessment of microplastics release from polyester fabrics: the impact of different washing conditions. *Environ Poll* 2020; 264: 113960.
27. Cai Y, Mitrano DM, Hufenus R, Nowack BJEs,. Formation of fiber fragments during abrasion of polyester textiles. *Environ Sci Techn* 2021; 55(12): 8001-9.
28. Zambrano MC, Pawlak JJ, Daystar J, Ankeny M, Cheng JJ, Venditti RA. Microfibers generated from the laundering of cotton, rayon and polyester based fabrics and their aquatic biodegradation. *Marin Poll Bullet* 2019; 142: 394-407.
29. Zambrano MC, Pawlak JJ, Daystar J, Ankeny M, Goller CC, Venditti RA. Aerobic biodegradation in freshwater and marine environments of textile microfibers generated in clothes laundering: Effects of cellulose and polyester-based microfibers on the microbiome. *Marin Poll Bullet* 2020; 151: 110826.
30. Ladewig SM, Bao S, Chow AT. Natural fibers: a missing link to chemical pollution dispersion in aquatic environments. *Environ Sci Techn* 2015; 49: 12609−10.

31. Cesa FS, Turra A, Baruque-Ramos J. Synthetic fibers as microplastics in the marine environment: a review from textile perspective with a focus on domestic washings. *Sci Total Environ* 2017; 598: 1116-29.
32. Periyasamy AP, Tehrani-Bagha A. A review of microplastic emission from textile materials and its reduction techniques. *Poly Degrad Stab* 2022;199:1-15.
33. Kim S, Cho Y, Park CH. Effect of cotton fabric properties on fiber release and marine biodegradation. *Text Res J* 2022;92:2121–37.
34. Engelhardt AW. Global development of spun and filament yarns. 2019 DECEMBER 4, 2019.
35. AG OSM. The Fiber Year 2009/10: A World Survey on Textile and Nonwovens Industry. 2010.
36. Hunter L. Cotton spinning technology. In: Gordon S, Hsieh YL, editors. *Cotton Science and Technology*: Woodhead Publishing; 2007. p. 240-74.
37. Lawrence CA. Fundamentals of Spun Yarn Technology (1st ed.): CRC Press; 2003.
38. Lawrence CA. Advances in Yarn Spinning Technology: Elsevier; 2010.
39. McNally JP, McCord FA. Cotton quality study: V: Resistance to abrasion. *Text Res J* 1960; 30(10): 715-51.
40. Raja Balasaraswathi S, Rathinamoorthy R. Effect of fabric properties on microfiber shedding from synthetic textiles. *J Text Inst* 2021; 113(5): 789-809.
41. Palacios-Marín AV, Jabbar A, Tausif M. Fragmented fiber pollution from common textile materials and structures during laundry. *Text Res J* 2022; DOI:10.1177/00405175221090971.
42. Berruezo M, Bonet-Aracil M, Montava I, Bou-Belda E, Díaz-García P, Gisbert-Payá J. Preliminary study of weave pattern influence on microplastics from fabric laundering. *Text Res J* 2021; 91(9-10): 1037-45.
43. Bresee RR, Annis PA, Warnock MM. Comparing Actual Fabric Wear with Laboratory Abrasion and Laundering. *Text Chem Color* 1994; 26(1): 17-23.
44. Militky J, Ibrahim S. Effect of textile processing on fatigue. *Fatigue failure of textile fibres*: Elsevier; 2009. p. 133-68.
45. Soltani P, Vadood M, Johari MSJF. Modeling spun yarns migratory properties using artificial neural network. *Fib Polym* 2012; 13(9): 1190-5.
46. Tyagi G. Yarn structure and properties from different spinning techniques. *Advances in Yarn Spinning Technology*: Elsevier; 2010. p. 119-54.

47. Soltani P, Johari M. A study on siro-, solo-, compact-, and conventional ring-spun yarns. Part I: structural and migratory properties of the yarns. *J Text Inst* 2012; 103(6): 622-8.
48. Buharali G, Omeroglu S. Comparative study on carded cotton yarn properties produced by the conventional ring and new modified ring spinning system. *Fib Text East Eur* 2019; 27: 45-51.
49. Soltani P, Johari M. A study on siro-, solo-, compact-, and conventional ring-spun yarns. Part II: yarn strength with relation to physical and structural properties of yarns. *J Text Inst* 2012; 103(9): 921-30.
50. Gupta B. Friction behavior of fibrous materials used in textiles. *Friction in Textile Materials*: Elsevier; 2008. p. 67-94.
51. Masen MA. A systems based experimental approach to tactile friction. *J Mech Behav Biomed Mater* 2011; 4(8): 1620-6.
52. Hearle JW, Lomas B, Cooke WD. *Atlas of fibre fracture and damage to textiles*. 2nd ed. England: Woodhead Publishing Ltd.; 1998.
53. Pinlova B, Hufenus R, Nowack B. Systematic study of the presence of microplastic fibers during polyester yarn production. *J Clean Prod* 2022; 363: 132247.
54. Yuksekkay ME. More about fibre friction and its measurements. *Text Prog* 2009; 41(3): 141-93.
55. El Gaiar M, Cusick G. A Study of the Morphology of Cotton-fibre Fracture in Abrasion Tests in Relation to the Coefficient of Friction between the Fabric Tested and the Abradant. *J Text Inst* 1976; 67(4): 141-5.
56. Textor T, Derksen L, Bahners T, Gutmann JS, Mayer-Gall T. Abrasion resistance of textiles: Gaining insight into the damaging mechanisms of different test procedures. *J Eng fib fab*. 2019;14:1-7.

Table 1. Properties of PIMA cotton fibres used in the study

Sr. No.	Parameters	Values
1	Upper Half Mean Length (mm)	37.008 ± 0.686
2	Fineness (micronaire)	4.58 ± 0.05
3	Tenacity (g⁄/Tex)	43.5 ± 0.6
4	Breaking Elongation (%)	6.9 ± 0.6
5	Uniformity Index (-)	87.8 ± 1.0
6	Short Fibre Index (%)	4.0 ± 0.1
7	Degree of Yellowness, +*b* (-)	13.7 ± 0.2
8	Degree of Reflectance, +*Rd* (-)	69.6 ± 0.6

Table 2. Properties of ring spun yarns

Sr. No.	Ring Spun Yarn	Actual count (tex)	Unevenness (%)	Total Imperfections /km	Hairiness Index (-)	Tenacity (cN/Tex)	Breaking Elongation (%)
1	Conventional	14.41±0.07	11.84±0.33	261±42	5.45±0.12	19.14±1.56	4.93 ± 0.38
2	Compact	14.89±0.11	11.29±0.18	231±33	5.07±0.04	21.98±2.48	5.41 ± 0.53
3	SIRO	15.21±0.03	11.73±0.70	286±62	4.68±0.14	21.78±1.84	5.70 ± 0.46

4	SIRO-compact	15.53±0.07	12.54±0.29	573±61	4.33±0.07	23.49±1.78	5.90 ± 0.34

Table 3. Significance values by Tukey's statistical analysis for comparison of FF mass release of normal with compact, SIRO and SIRO-compact fabrics

Variable	By	Abrasion and laundering cycle					
		1	2	3	4	5	6
Specimen							
Conventional (FF mass, mg/g)	Compact (FF mass, mg/g)	0.001*	0.017*	0.024*	0.000*	0.001*	0.192
	SIRO (FF mass, mg/g)	0.000*	0.009*	0.036*	0.000*	0.000*	0.960
	SIRO compact (FF mass, mg/g)	0.000*	0.008*	0.011*	0.000*	0.004*	0.660
Abradant							
Conventional (FF mass, mg/g)	Compact (FF mass, mg/g)	0.000*	0.228	0.904	0.028*	0.053	0.002*
	SIRO (FF mass, mg/g)	0.000*	0.061	0.959	0.093	0.012*	0.053
	SIRO compact (FF mass, mg/g)	0.000*	0.434	0.289	0.092	0.010*	0.138

**Statistically significant with 95% confidence level.*

Table 4. Significance values from student's t-test for statistical significance of tensile properties of yarns and surface properties of textile samples before and after the abrasion & laundering cycles.

Variable	Tensile properties of yarns		Kawabata fabric surface properties	
	Tensile strength (cN/tex)	Elongation (%)	MIU (-)	SMD (μm)
Conventional	0.018*	0.009*	0.009*	0.058
Compact	0.000*	0.032*	0.001*	0.341
SIRO	0.057	0.001*	0.033*	0.304
SIRO-compact	0.786	0.000*	0.008*	0.401

**Statistically significant with 95% confidence level.*

Figure captions

Figure 1. Schematic representation of yarn formation principles during ring spinning (dimensions not to scale).

Figure 2. Textiles dyeing procedure

Figure 3. The Martindale abrasion with a modified experimental setup.

Figure 4. FF mass collected from wash effluent after abrasion & laundering of abraded Specimens and Abradants.

Figure 5. (a) Tensile strength and (b) breaking elongation of yarns before 1st and after 6th cycles of abrasion & laundering.

Figure 6. (a) Coefficient of surface friction and (b) surface roughness of Abradants before 1st and after 6th cycles of abrasion & laundering.

Figure 7. Light microscopic images of (a) normal, (b) compact, (c) SIRO and (d) SIRO-compact textiles samples after 6th abrasion & laundering cycle.

Figure 8. Characterisation of fractured fibre ends released from Conventional sample after (a) 1st cycle and (b) 6th cycle of abrasion & laundering.

Figure 9. Characterisation of fractured fibre ends released from SIRO-compact sample after (a) 1st cycle and (b) 6th cycle of abrasion & laundering.

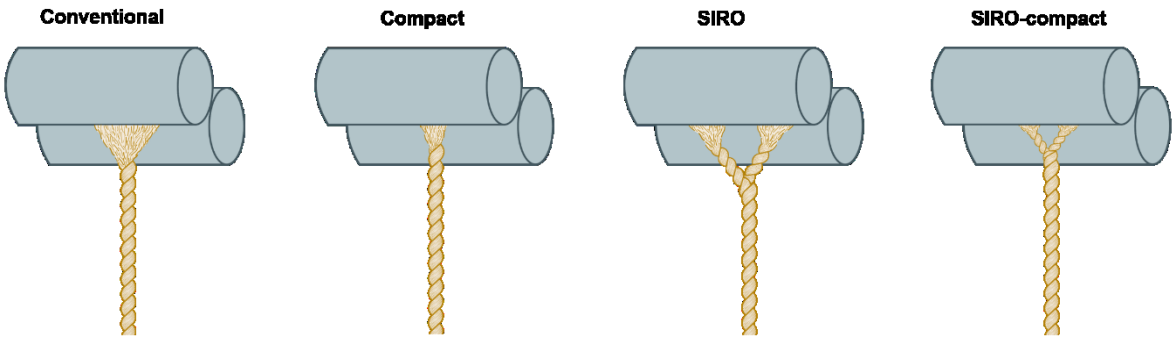

Figure 1. Schematic representation of yarn formation principles during ring spinning (dimensions not to scale).

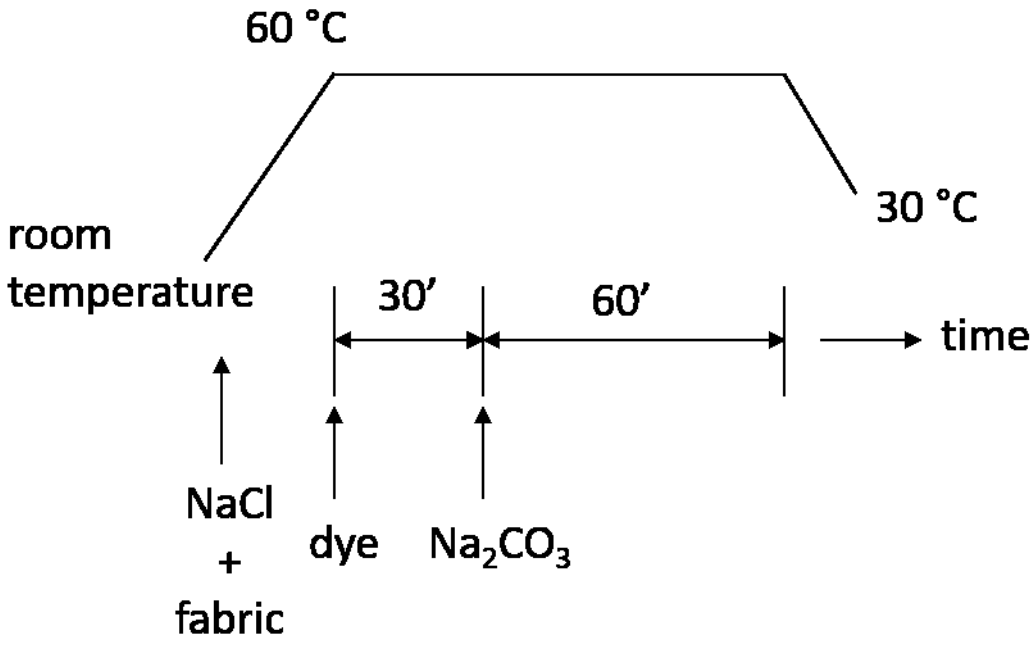

Figure 2. Textiles dyeing procedure

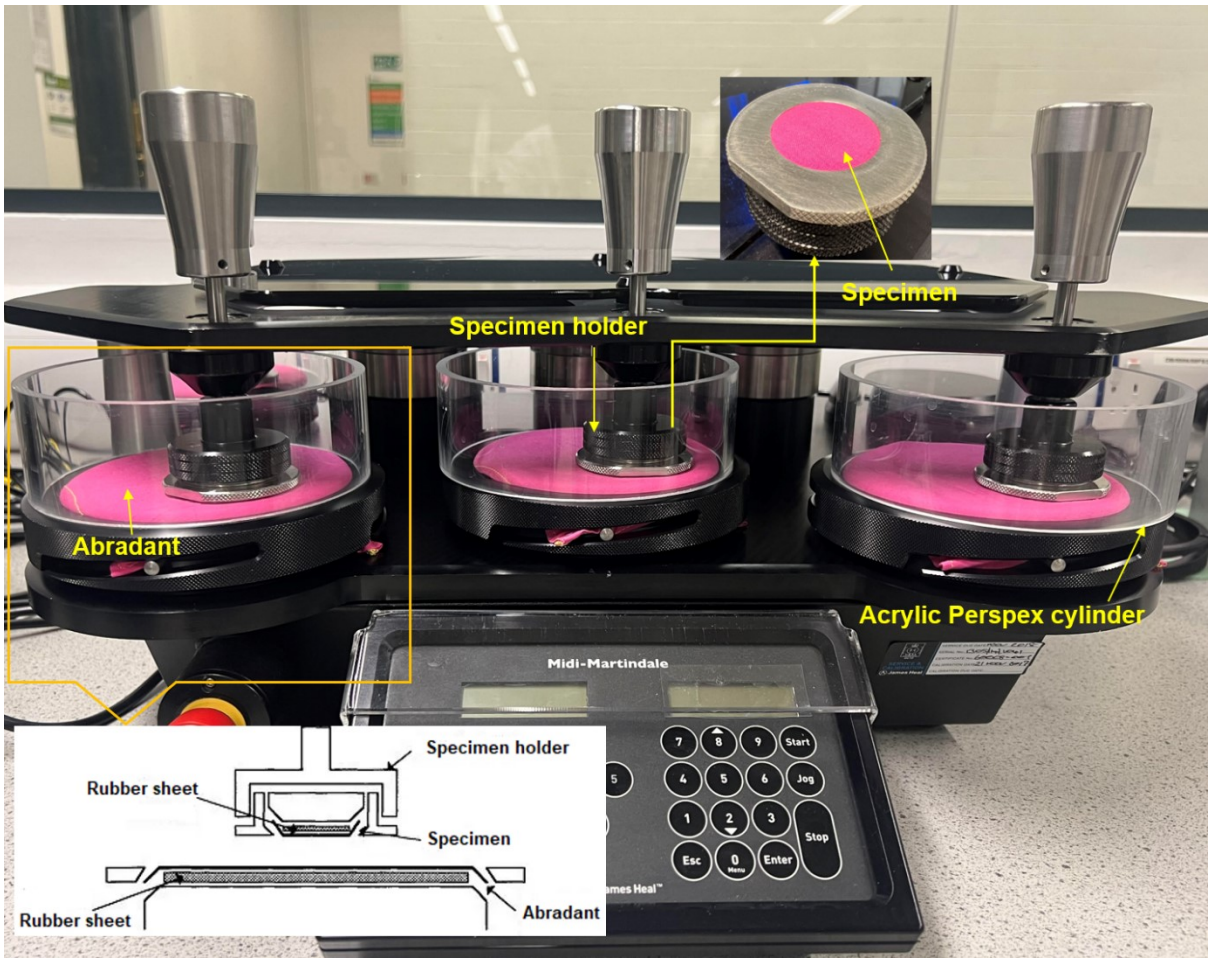

Figure 3. The Martindale abrasion with a modified experimental setup.

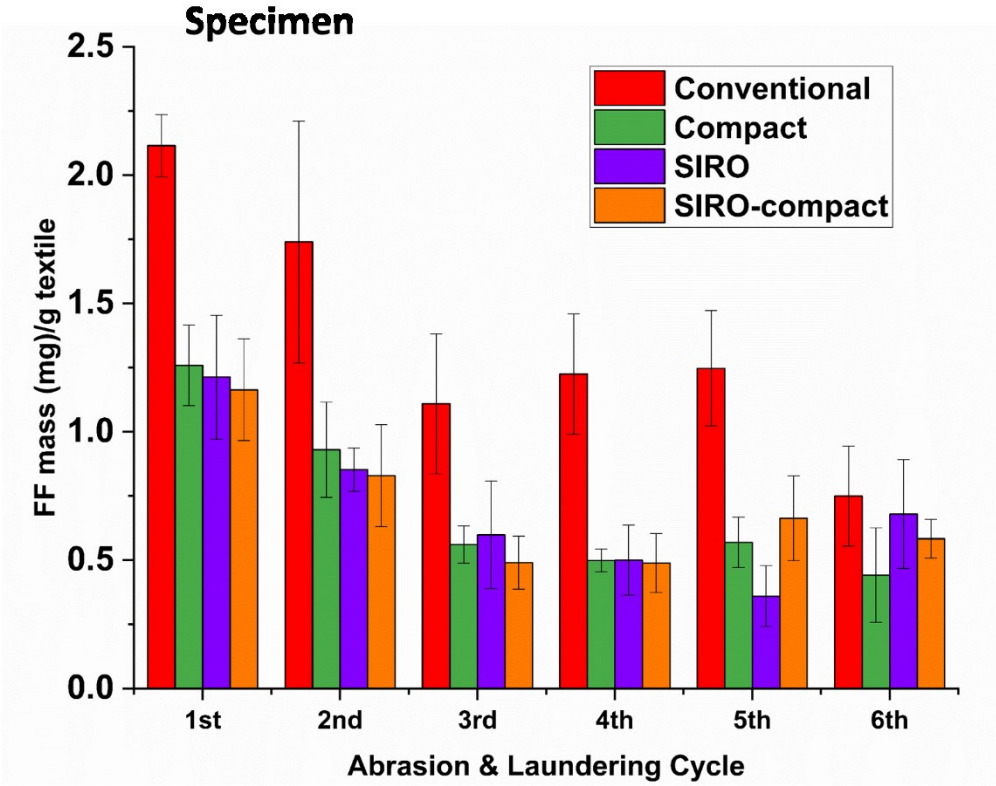

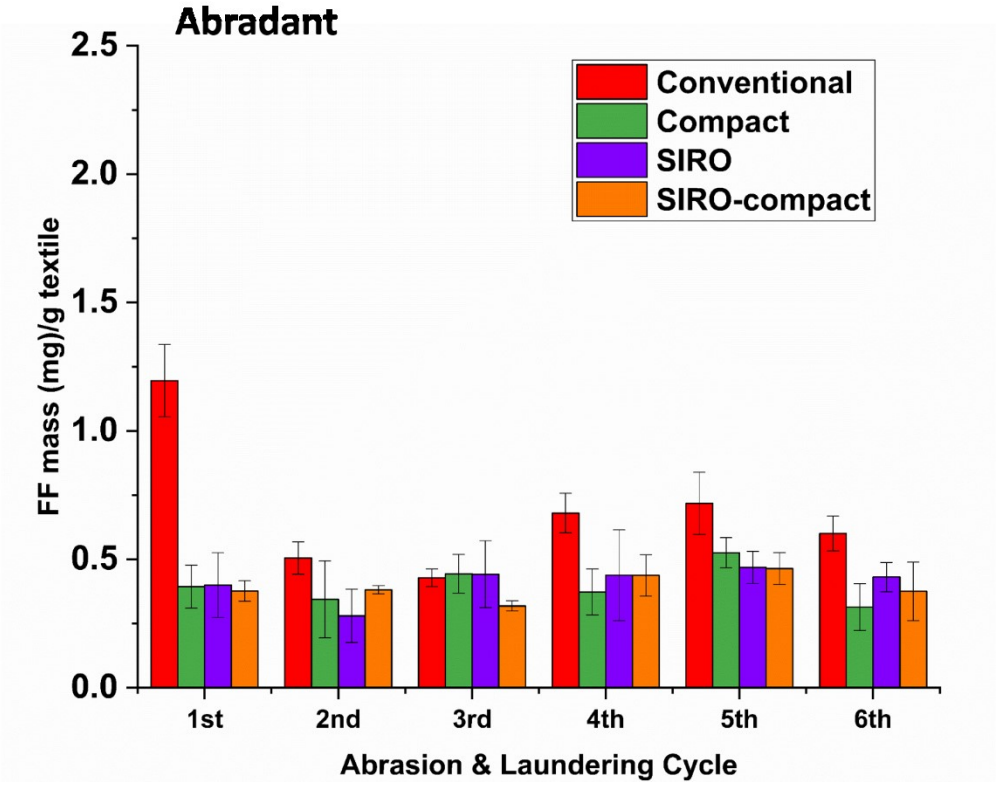

Figure 4. FF mass collected from wash effluent after abrasion & laundering of abraded Specimens and Abradants.

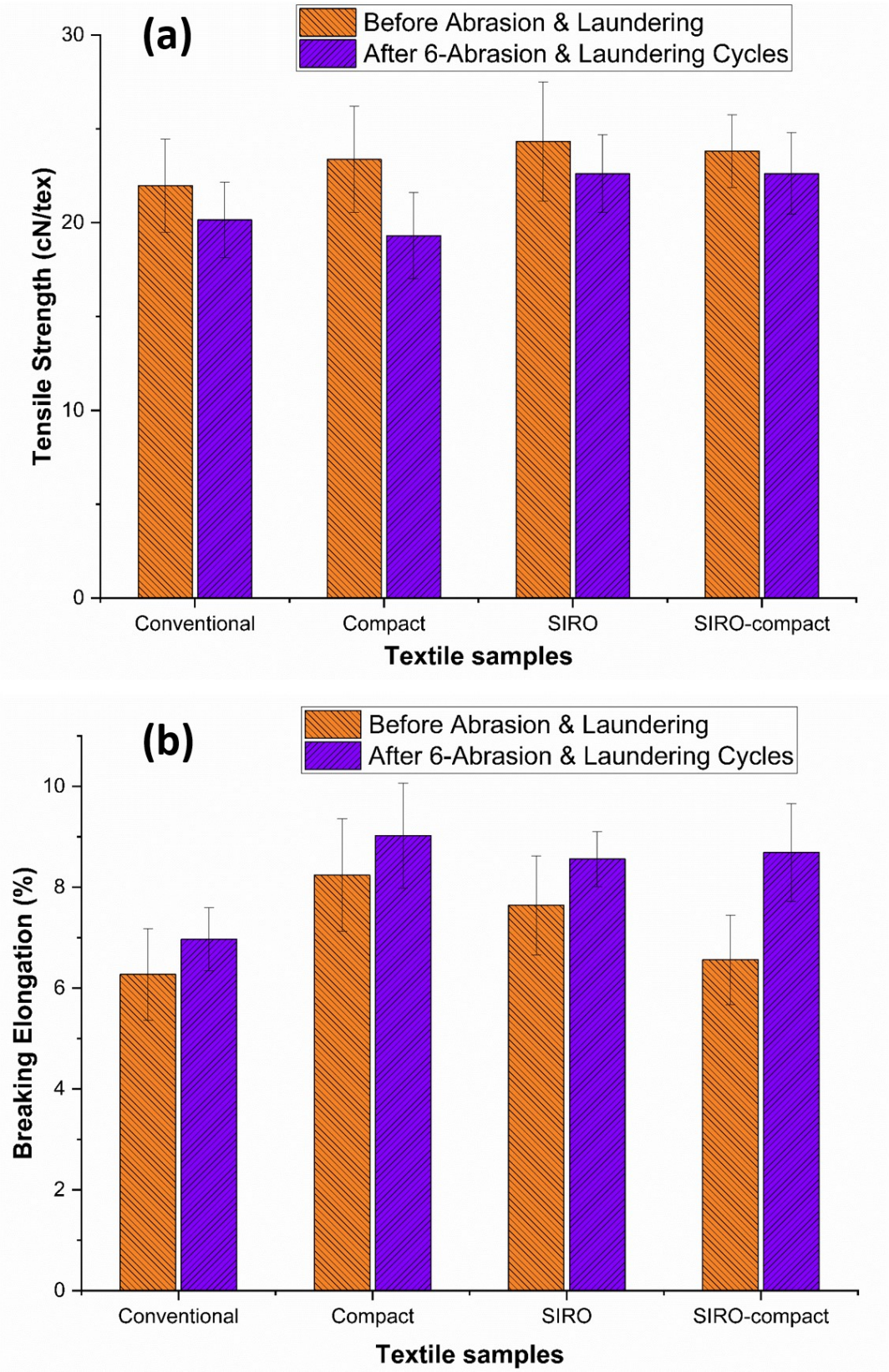

Figure 5. (a) Tensile strength and (b) breaking elongation of yarns before 1st and after 6th cycles of abrasion & laundering.

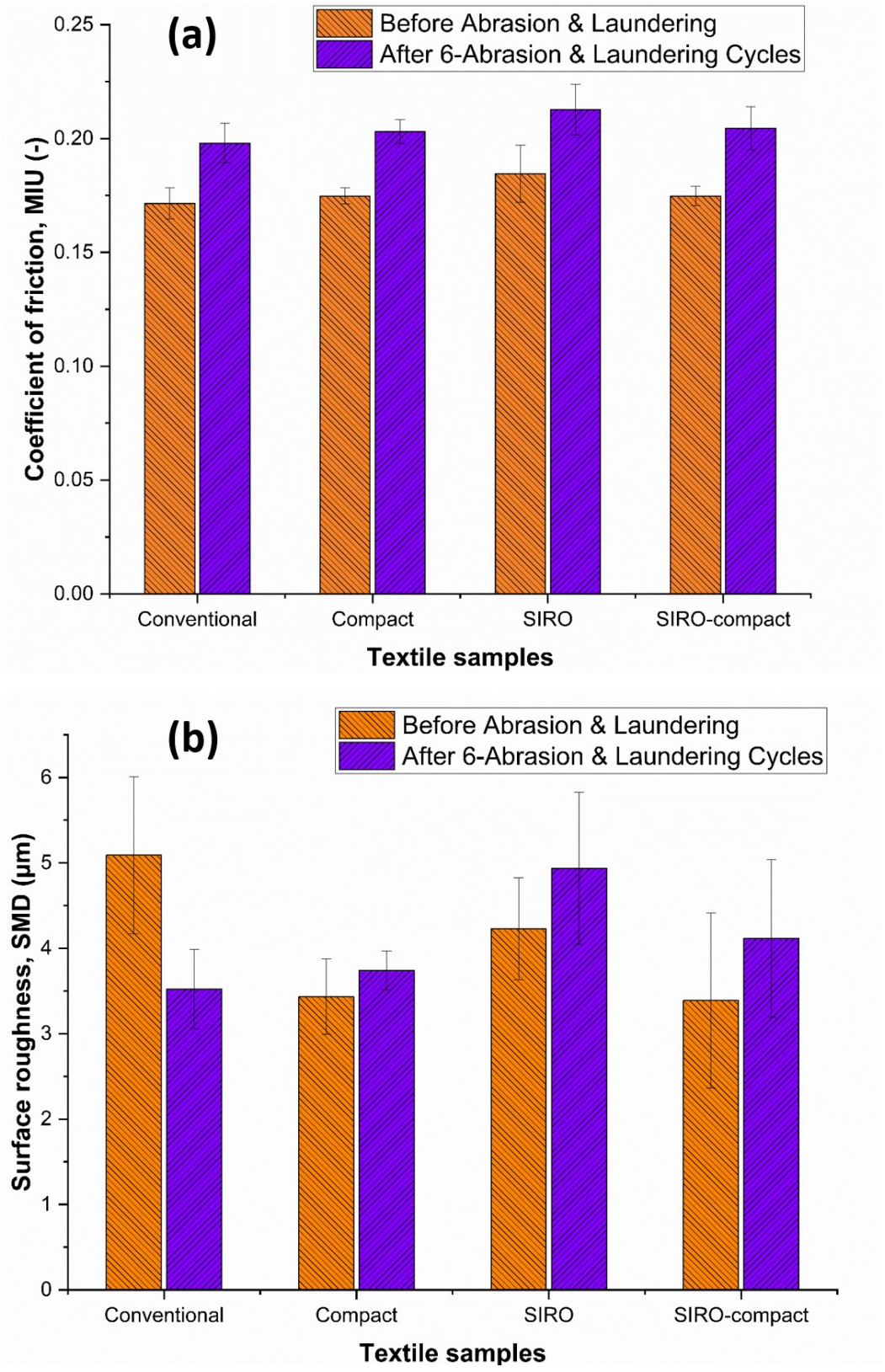

Figure 6. (a) Coefficient of surface friction and (b) surface roughness of Abradants before 1st and after 6th cycles of abrasion & laundering.

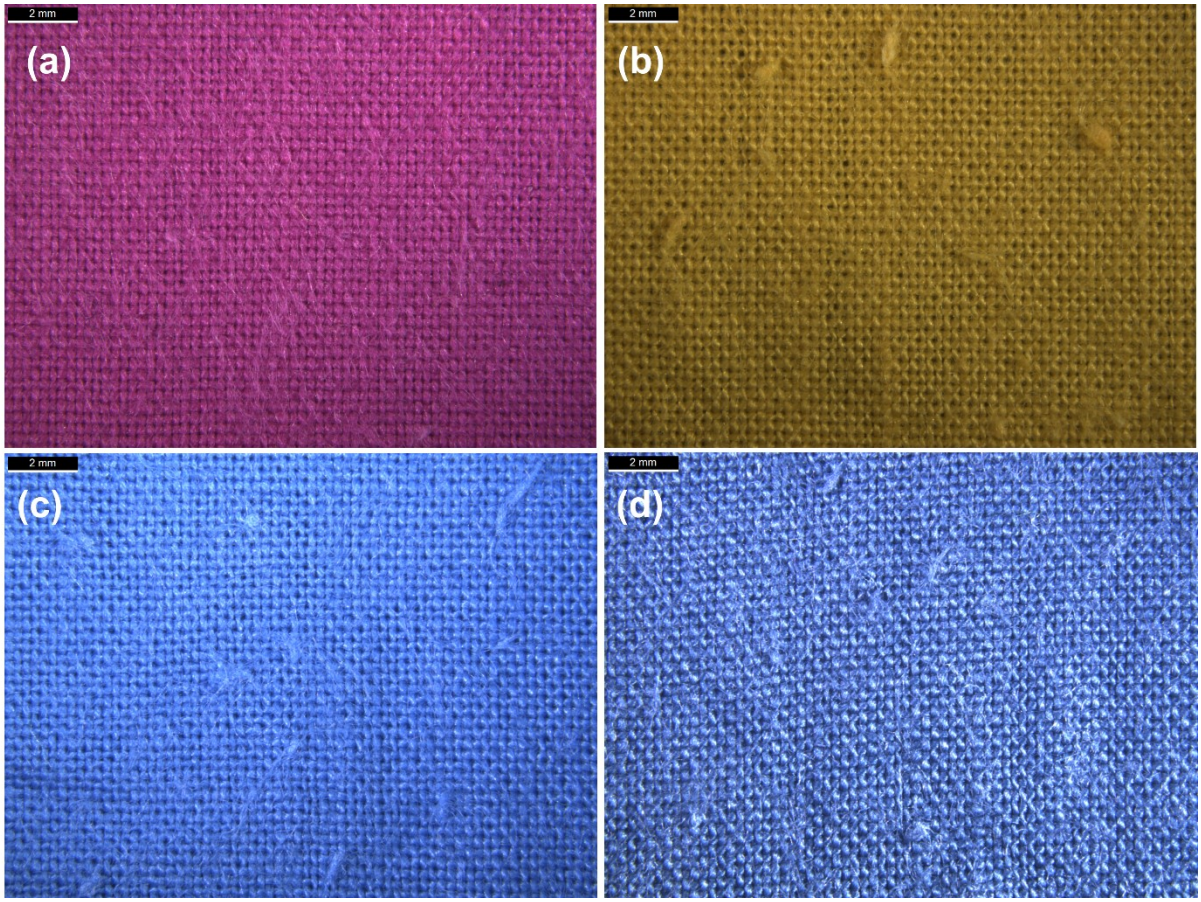

Figure 7. Light microscopic images of (a) normal, (b) compact, (c) SIRO and (d) SIRO-compact textiles samples after 6th abrasion & laundering cycle.

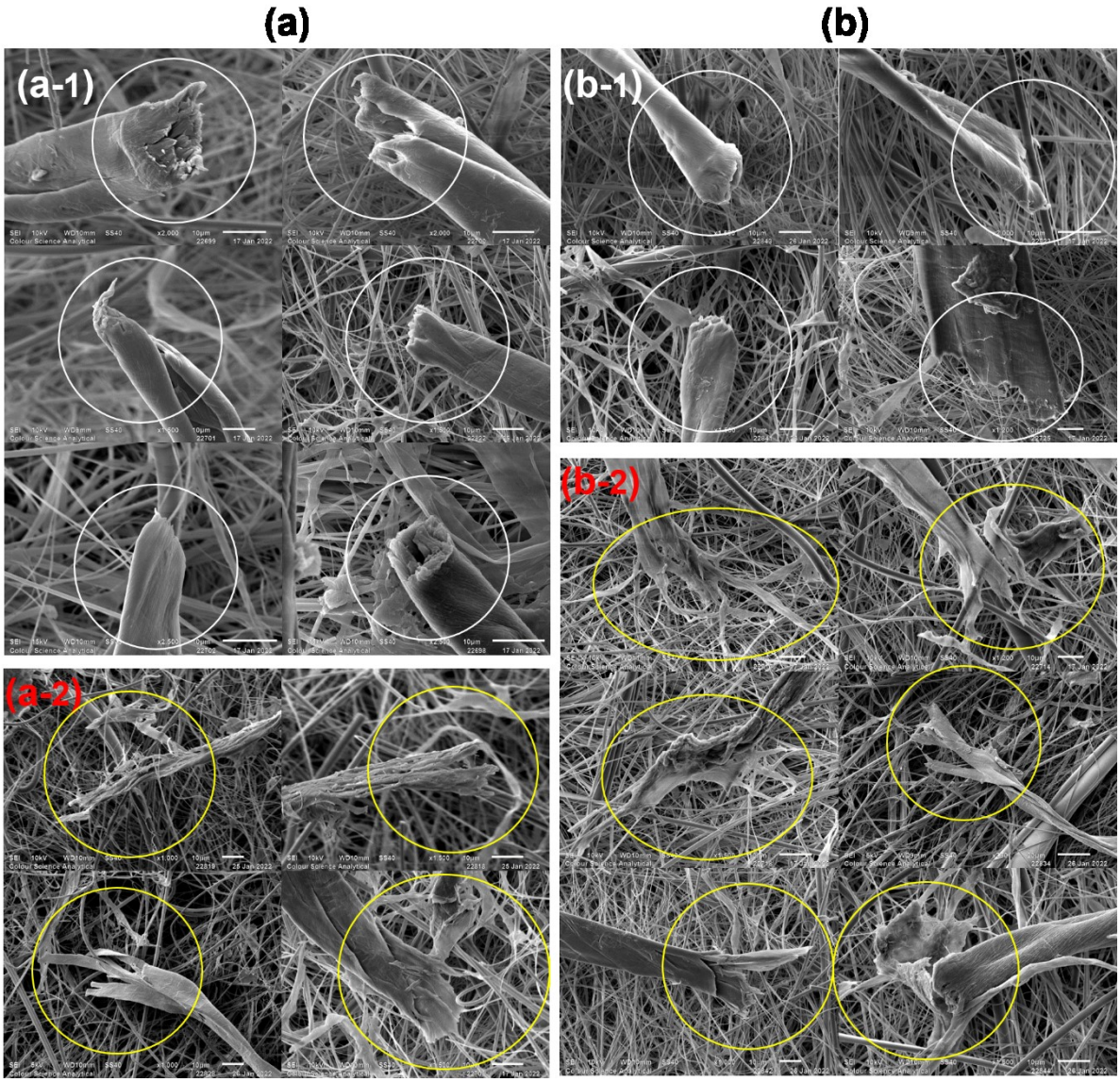

Figure 8. Characterisation of fractured fibre ends released from Conventional sample after (a) 1st cycle and (b) 6th cycle of abrasion & laundering.

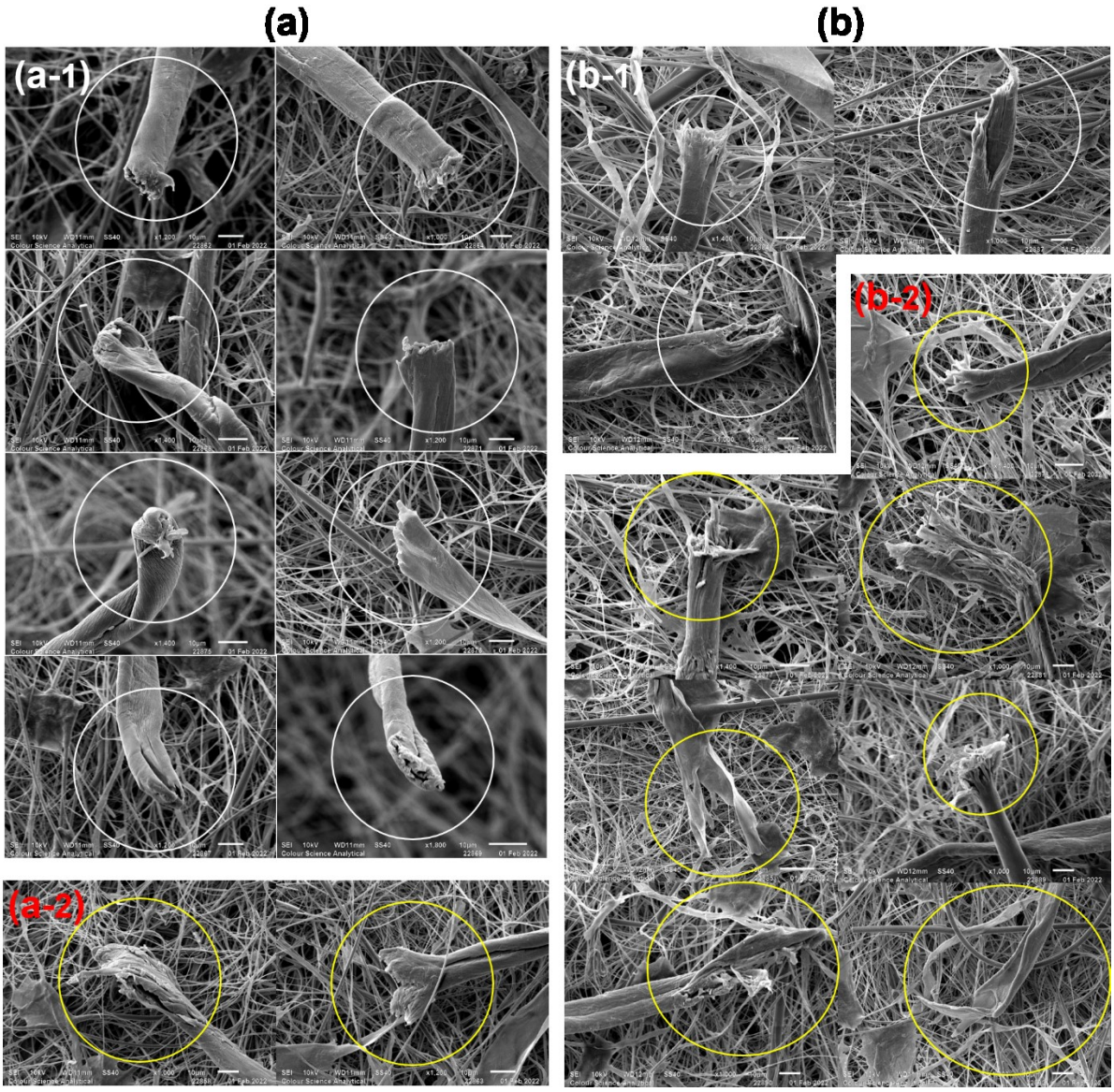

Figure 9. Characterisation of fractured fibre ends released from SIRO-compact sample after (a) 1st cycle and (b) 6th cycle of abrasion & laundering.